XVI SIMPOSIO
IBEROAMERICANO
SOBRE PROTECCIÓN
DE SISTEMAS ELÉCTRICOS
DE POTENCIA

A differential transformer protection based-on energy modes

Ernesto Vázquez[a], Manuel A. Andrade[a], Héctor Esponda[b], Daniel Guillén[c]

[a]*Universidad Autónoma de Nuevo León*
[b]*National Energy Control Center (Independent System Operator)*
[c]*Tecnologico de Monterrey*

A B S T R A C T

A novel algorithm for improved differential protection of power transformers is presented in this paper. The algorithm uses as the difference of energies contained in the greatest singular value of the instantaneous differential and restraint currents through the singular value decomposition (SVD) as a basis. From the difference of energies, the accumulated numerical integration is calculated to reduce the impact of the current transformer (CT) saturation. Then, the differentiation sample to sample of the accumulated numerical integration is obtained with the goal to detect abrupt changes in the difference of energies. If the differentiation has a slope higher than 45°, the algorithm will detect an internal fault. Otherwise, the algorithm will identify either a steady-state condition or a transient event such as an inrush current, an external fault or an overexciting. The algorithm was developed in MATLAB software and tested using signals from an electromagnetic transient software. The algorithm showed a successful discrimination in all tested events.

Keywords: Power transformer, differential protection, energy, singular value decomposition, slope

1. Introduction

When a power transformer is energized, the transient phenomenon well-known as magnetizing inrush current will take place. This phenomenon has been widely addressed by researchers to avoid the misoperation of the conventional percentage differential protection when this event occurs. New methods should have the ability to discriminate between internal faults and transient conditions caused by external events or by disturbances associated with the measurement devices such as noise, and errors in current transformers (CTs)[1]. In this sense, the need of developing robust protection methods to detect internal faults in transformers is essential to maintain reliable power delivery.

Several methods have been developed to ensure the correct operation of the differential protection scheme. The harmonic content of the inrush current signal has been taken as one of the principal indicators to detect when inrush current occurs[2–4]. However, the newest transformers are manufactured with magnetic steels that reduce the losses of the transformer core. As a result, the harmonic content of the inrush current also has decreased[5]. In[6], the Empirical Fourier transform based on the discrete Fourier transform is used as the basis to discriminate transient events from internal faults. However, the method was not tested on remanent flux conditions.

Superimposed differential currents are presented in[7] to establish a protection scheme for power transformers. The method is based on the obtaining of the positive and negative sequences of the differential currents once the superimposed component of the differential currents has been extracted. Nevertheless, the principal challenge this method faces is to detect three-phase faults which have the reduced negative sequence component. Other approaches based on negative sequence have been proposed[8]. A method based on the non-saturation zone of the inrush currents is introduced in[9]. The method uses the sum of the first quarter of the typical characteristic of the valley or dead angle zone of the inrush currents to differentiate between a fault and an inrush current. However, the use of an empirical threshold and the high computational burden are the disadvantages of the method. In[10], a method based on the mathematical morphology is presented. This image processing tool extracts the main waveform features of the differential currents using the erosion and dilation morphological operations. Nevertheless, the thresholds were established using empirical values. In[11], a method based on the ratio of the absolute sum and absolute difference of the primary and secondary currents and voltages is presented. However, the identification threshold was determined on simulation results.

Emails: evazquezmtz@gmail.com (Ernesto Vázquez), manuel.andradest@uanl.edu.mx (Manuel A. Andrade), hector.esponda@cenace.gob.mx (Héctor Esponda), guillenad@tec.mx (Daniel Guillén)

The wavelet transform is a powerful technique used in different methods[12–15] to correctly discriminate internal faults from inrush currents. Frequency bands are used for the methods to extract the most energy of the differential currents depending on the number of coefficients selected. Nevertheless, the main drawback of these methods is the high computational burden. Also, there are some points must be considered such as the selection of the mother wavelet, the need to compensate for the negative effects of the noise and CT saturation, and a pickup threshold to detect the transient event. Statistical distribution has been utilized in different methods to discriminate inrush currents from faults. In[16–18], the second central moment is proposed to characterize the inrush current waveform in a power transformer based on the similarity to a half-sinusoidal signal. The discrimination of the event was made using a threshold that sets the maximum variance that a half-sinusoidal waveform could achieve. The method does not depend on the transformer or grid parameters. In this sense, a method based on the fourth central moment, known as the kurtosis, to characterize the features of the inrush current is presented in[19]. Nevertheless, the detection threshold must be recalculated if the power system is modified. Other method based on statistic analysis was proposed in[20], where the waveforms of non-fault and fault conditions were characterized to ensure the protection performance under transient events.

In this paper, an algorithm based on the difference of the energies of the instantaneous differential and restraint currents using the SVD is proposed. The proposed algorithm obtains the greatest singular value of the differential and restraint currents once the signals are filtered and normalized. The filtering and normalization stages are applied to generalize the algorithm to any transformer without depending on the transformer parameters, and to highlight changes in the differential and restraint currents. To avoid the negative impact of some factors such as the CT saturation and noise, the numerical integration is calculated from the differences of energies. Finally, to speed up the fault detection time, the differentiation of the numerical integration is determined and compared to the discrimination threshold.

2. Mathematical foundations

Nowadays, the measurement data from any phenomenon is discretized. This measured information can be organized in an $m \times n$ matrix X where m is the number of observations and n is the number of the variables as follows:

$$X = \begin{bmatrix} x_{11} & x_{12} & \cdots & x_{1n} \\ x_{21} & x_{22} & \cdots & x_{2n} \\ \vdots & \vdots & \ddots & \vdots \\ x_{m1} & x_{m2} & \cdots & x_{mn} \end{bmatrix} \tag{1}$$

From a statistical view, the linear relationship between variables and observations may bring relevant information when a disturbance occurs. This relation can be obtained using an $n \times n$ variance-covariance matrix Σ with zero mean[21], defined as:

$$\Sigma = \frac{1}{n} X X^T \tag{2}$$

where n is the number of observations. However, the covariance matrix has a high computational cost[22]. Nevertheless, an alternative to obtaining an estimate of the data behavior is possible using the singular value decomposition (SVD)[23]. The estimation of the variance-covariance matrix can be obtained using only the left singular value as follows:

$$\tilde{\Sigma} = \tfrac{1}{n} U S^2 U^T \tag{3}$$

where n is the number of samples, S is a diagonal $m \times n$ matrix that contains the singular values (also called modes), and U and V are the orthogonal right and left eigenvectors, respectively.

If the trace of (3) is compared with the trace of (2) obtained directly from the data matrix X, they will be equivalent. Therefore, the sum of the variance of original variables and the sum of the modes divided into the number of samples from the estimated variance are equivalents. Therefore, the information provided for the modes represent the information of the original variable data with an acceptable computational cost[24]. In this sense, the modes provide the energy of the original variables[25,26]. Thus, if most of the energy from the original measurement data are required, the greatest singular value (GSV) must be selected.

2.1. Application in a transformer differential protection

The information provided by the GSV can be used to extract the energy of the instantaneous operation I_{op} and restraint current I_{rest} defined as:

$$I_{\text{opABC}} = I_p + I_s \tag{4}$$

$$I_{\text{restABC}} = I_p - I_s \tag{5}$$

where I_p and I_s are the CT secondary currents from the high and low voltage side, respectively. The goal is to obtain the most energy from the operation and restraint current and to compare their behavior. The energy mode of the operation currents is defined as:

$$\Lambda I_{\text{opABC}} = \text{svd}\left(I_{\text{opABC}}\right) \tag{6}$$

$$\Lambda I_{\text{opABC}} = \frac{1}{n} U_{\text{op}} S_{\text{op}}^2 U_{\text{op}}^T \tag{7}$$

$$\Lambda I_{\text{opABC}} = \frac{1}{n} \begin{bmatrix} \lambda_{\text{op1}} & 0 & 0 \\ 0 & \lambda_{\text{op2}} & 0 \\ 0 & 0 & \lambda_{\text{op3}} \end{bmatrix}^2 \tag{8}$$

$$\lambda I_{\text{opABC}} = \frac{1}{n} \left(\lambda_{\text{op1}}\right)^2 \tag{9}$$

and the energy mode of the restraint currents is defined as:

$$\Lambda I_{\text{restABC}} = \text{svd}\left(I_{\text{restABC}}\right) \tag{10}$$

$$\Lambda I_{\text{restABC}} = \frac{1}{n} U_{\text{rest}} S_{\text{rest}}^2 U_{\text{rest}}^T \tag{11}$$

$$\Lambda I_{\text{restABC}} = \frac{1}{n} \begin{bmatrix} \lambda_{\text{rest1}} & 0 & 0 \\ 0 & \lambda_{\text{rest2}} & 0 \\ 0 & 0 & \lambda_{\text{rest3}} \end{bmatrix}^2 \tag{12}$$

$$\lambda I_{\text{restABC}} = \frac{1}{n} \left(\lambda_{\text{rest1}}\right)^2 \tag{13}$$

where λ_{IopABC} and $\lambda_{\text{IrestABC}}$ represent the energy modes of the operation and restraint current through the magnitude of the greatest singular value obtained from the SVD decomposition.

Initial tests to provide an example of this concept were applied to a power transformer as shown in Fig. 1. An inrush current and a single-phase fault inside the differential protection zone were simulated as is illustrated in Fig. 1(a) and Fig. 1(b), respectively. The magnitudes of the energy modes of λ_{IopABC} and $\lambda_{\text{IrestABC}}$ of both events are illustrated in Fig. 1(c) and Fig. 1(d). The comparison demonstrates the magnitude of the mode $\lambda_{\text{IrestABC}}$ was greater than the magnitude of the mode λ_{IopABC} when the inrush current occurred. On the other hand,

when the internal fault happened, the magnitude of the mode λ_{IopABC} was higher than the magnitude of the mode $\lambda_{\text{IrestABC}}$. Based on these and all results obtained previously (including the cases discussed later in this paper), a new differential protection concept based on the difference of the energy modes of the operation (λ_{IopABC}) and restraint current ($\lambda_{\text{IrestABC}}$) is proposed:

$$\Lambda_{87\text{TDEM}} = \lambda_{\text{IopABC}} - \lambda_{\text{IrestABC}} \tag{14}$$

where $\Lambda_{87\text{TDEM}}$ is defined as the Differential Energy Mode (DEM). In steady-state Λ_{87TDEM} will be equal, or nearly equal to zero because of the current balance according to the Kirchoff Current Law. However, if an inrush current occurs, $\Lambda_{87\text{TDEM}}$ will take negative values as is shown in Fig. 1(e). On the other hand, if an internal fault happens, the magnitude of $\Lambda_{87\text{TDEM}}$ will have a positive magnitude as is shown Fig. 1(f). Therefore, the $\Lambda_{87\text{TDEM}}$ can be used to differentiate transient conditions such as inrush currents, external faults, and overexciting from faults inside the differential protection based on the sign of $\Lambda_{87\text{TDEM}}$.

3. Proposed Algorithm

The algorithm is formed over three different stages, as the flowchart shows in Fig. 2. These stages are data acquisition (stage 1), processing signal (stage 2), and energy mode calculation (stage 3). Every stage will be explained as follows.

3.1. Data acquisition (stage 1)

The algorithm uses the instantaneous operation and restraint currents as the input signals to the algorithm. These signals are formed with the CT secondary currents phase-shifted compensated from the primary and secondary side of the power transformer, respectively. The operation I_{opABC} and restraint I_{restABC} currents are defined as:

$$I_{\text{opABC}} = I_{px} + I_{sx} \tag{15}$$

$$I_{\text{restABC}} = I_{px} - I_{sx} \tag{16}$$

where I_{px} and I_{sx} are the CT secondary currents from the HV and LV, and x = A, B, C corresponds to each phase.

3.2. Processing signal (stage 2)

3.2.1. Sliding window

Once, the operation and restraint currents are obtained, the algorithm organizes this information using two sliding windows as is shown:

$$I_{\text{opABC}} = \begin{bmatrix} I_{\text{opA}_1} & I_{\text{opB}_1} & I_{\text{opC}_1} \\ \vdots & \vdots & \vdots \\ I_{\text{opA}_{32}} & I_{\text{opB}_{32}} & I_{\text{opC}_{32}} \\ \vdots & \vdots & \vdots \\ I_{\text{opA}_{64}} & I_{\text{opB}_{64}} & I_{C\,\text{op64}} \end{bmatrix}_{\text{m}\times\text{n}} \tag{17}$$

$$I_{\text{restABC}} = \begin{bmatrix} I_{\text{restA}1} & I_{\text{restB}1} & I_{\text{restC}1} \\ \vdots & \vdots & \vdots \\ I_{\text{restA}32} & I_{\text{restB}32} & I_{\text{restC}32} \\ \vdots & \vdots & \vdots \\ I_{\text{restA}64} & I_{\text{restB}64} & I_{\text{restC}64} \end{bmatrix}_{\text{m}\times\text{n}} \tag{18}$$

where I_{opA}, I_{opB}, I_{opC}, I_{restA}, I_{restB}, and I_{restC} are the operation and restraint currents for phases A, B, and C, respectively. The sliding window has a dimension of ($m = 64 \times n = 3$), where they correspond to 64 samples/cycle for each differential and restraint current. This sampling frequency was selected to match a rate used in many digital relays. However, the algorithm can be applied using any sampling frequency. This signal processing routine results in an algorithm that does not require setting a minimum pickup threshold.

3.2.2. Filtering

The algorithm filters the operation and restraint currents to eliminate any redundant information. The filtering is carried out using a Delta filter[27]. This filter is based on superimposed (incremental) quantities and uses transient measurements to remove the pre-fault conditions and the periodicity of the signals, highlighting any change that may occur in I_{opABC} and I_{restABC}. The result of the application of the Delta filter to the operation and restraint currents are the incremental operation current ΔI_{opABC}, and the incremental restraint current $\Delta I_{\text{restABC}}$, defined as:

$$\Delta I_{\text{opABC}}(i) = I_{\text{opABC}}(i) - I_{\text{opABC}}(i - nT) \tag{19}$$

$$\Delta I_{\text{restABC}}(i) = I_{\text{restABC}}(i) - I_{\text{restABC}}(i - nT) \tag{20}$$

where i represents the present sample, and nT is the number of periods of the fundamental frequency. For this application, $nT = 1$.

3.2.3. Normalization

To generalize the application of the algorithm to any transformer regardless of the rating, saturation curve, connection, and the transformer parameters, the incremental operation and incremental restraint currents must be normalized. The normalization will scale the signals between the range $[-1, +1]$. The normalization subtracts the mean value of the actual window and divides all the samples (for window) by the maximum absolute value in each window as:

$$\Delta I_{\text{opABC N}}(i) = \frac{\Delta I_{\text{opABC}}(i) - \text{mean}\left(\Delta I_{\text{opABC}}(i)\right)}{\left|\max(\Delta I_{\text{opABC}})\right|} \tag{21}$$

$$\Delta I_{\text{restABC N}}(i) = \frac{\Delta I_{\text{restABC}}(i) - \text{mean}\left(\Delta I_{\text{restABC}}(i)\right)}{\left|\max(\Delta I_{\text{opABC}})\right|} \tag{22}$$

where i is the present sample, $\left|\max(\Delta I_{\text{opABC}})\right|$, and $\left|\max(\Delta I_{\text{restABC}})\right|$ are the maximum absolute values in each window of the incremental operation and incremental restraint current, respectively, and $\Delta I_{\text{opABC N}}$ and $\Delta I_{\text{restABC N}}$ are the normalized incremental operation and normalized incremental restraint currents, respectively.

3.3. Energy mode calculation (stage 3)

3.3.1. Calculation of $\Lambda_{87\text{TDEM}}$ index

The algorithm applies the SVD using (3) to obtain the squared largest singular value divided into the number of samples of each window of the normalized incremental operation currents (21) and the normalized incremental restraint currents (22) as:

$$\lambda I_{\text{opABC}} = \frac{1}{n}\left(\lambda_{1\Delta I_{\text{opABC N}}}\right)^2 \tag{23}$$

$$\lambda I_{\text{restABC}} = \frac{1}{n}\left(\lambda_{1\Delta I_{\text{restABC N}}}\right)^2 \tag{24}$$

where λI_{opABC} and $\lambda I_{\text{restABC}}$ represent the energy modes of the normalized incremental operation and restraint currents, respectively. The number of samples selected is $n = 64$. Then, the Λ_{87TDEM} index is calculated as:

$$\Lambda_{87\text{TDEM}}(i) = \lambda I_{\text{opABC}}(i) - \lambda I_{\text{restABC}}(i) \tag{25}$$

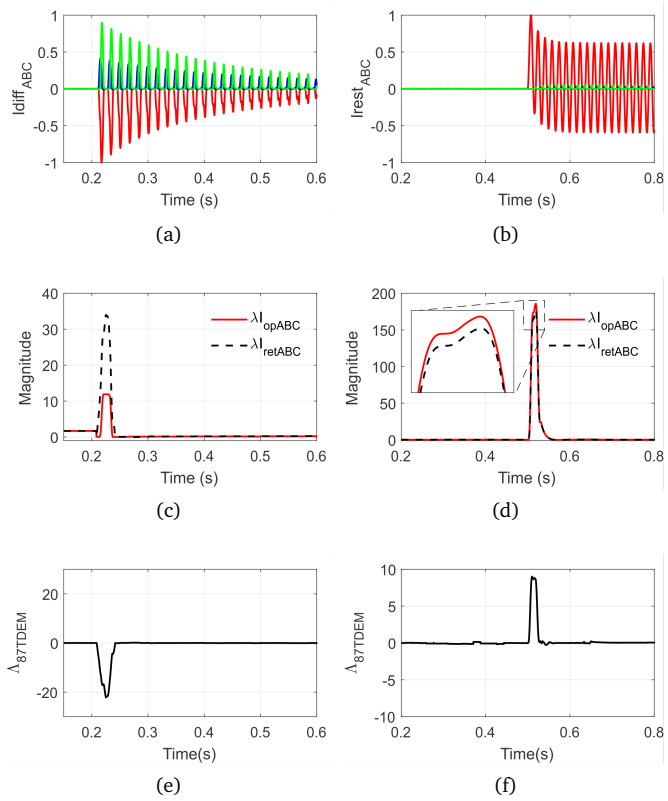

Fig. 1. Behavior of the energy modes of the operation and restraint currents during an inrush and fault current: (a) Inrush current waveform, (b) fault current waveform, (c) comparison between the operation and restraint energy modes in an inrush current, (d) comparison between the operation and restraint energy modes in a fault current, (e) magnitude of the Λ_{87TDEM} during an inrush current, and (f) magnitude of the Λ_{87TDEM} during an internal fault.

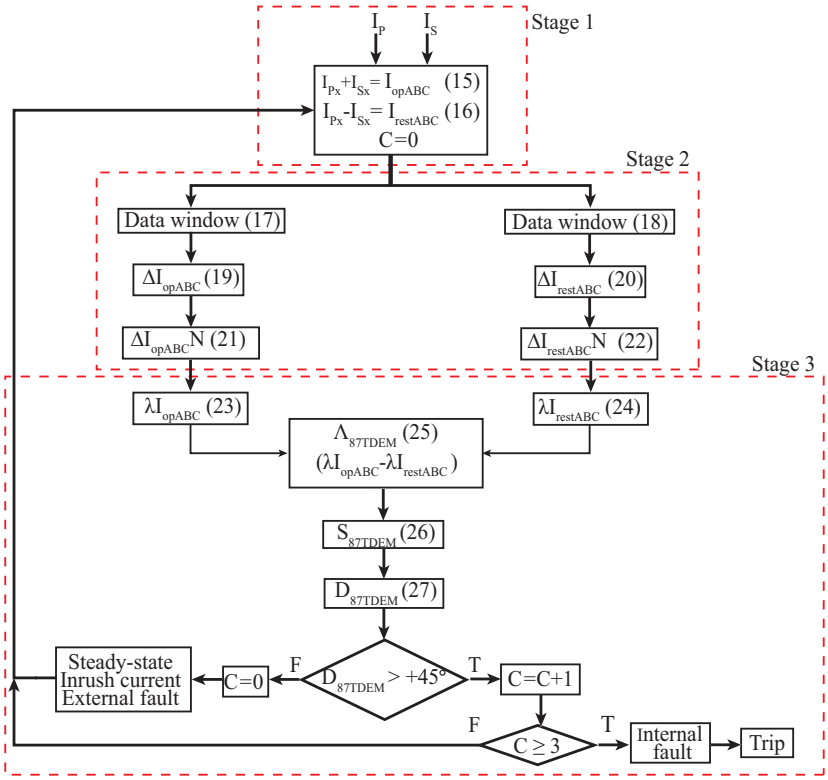

Fig. 2. Flowchart for the proposed algorithm.

In steady-state, Λ_{87TDEM} will be equal to zero, but in case of an inrush current, Λ_{87TDEM} will take negative values. On the other hand, if an internal fault occurs, Λ_{87TDEM} will have positive values higher than zero. Therefore, the sign of the magnitude of Λ_{87TDEM} can be used to discriminate between transient conditions where the element should block (inrush currents, external faults, overexcitation) and internal faults.

3.3.2. Calculation of S_{87TDEM} index

CT saturation is one of the main factors that may cause the misoperation of the differential elements. Therefore, the S_{87TDEM} index was introduced to reduce the issues caused by the CT saturation. The S_{87TDEM} index is defined as the numerical integration of the Λ_{87TDEM} index as is shown:

$$S_{87TDEM}(i) = \frac{\Delta t}{2}\sum_{i=1}^{N}\left(\Lambda_{87TDEM}(i) + \Lambda_{87TDEM}(i+1)\right) \quad (26)$$

where Δt is the sampling time (at 64 samples per 60 Hz cycle), and N is the length of the window. In steady-state, the S_{87TDEM} will take values around zero. If a transient event not associated with an in internal fault happens, the S_{87TDEM} will achieve negative values depending on the sign and magnitude of the Λ_{87TDEM} index, but it will remain on negative values until another event occurs. On the other hand, if an internal fault has a place, the S_{87TDEM} will assume positive values.

3.3.3. Calculation of D_{87TDEM} index

To speed up the fault detection time when an internal fault has been detected, the D_{87TDEM} index is calculated. The D_{87TDEM} index is defined as the numerical differentiation of the S_{87TDEM} on a sample to sample basis, as is shown:

$$D_{87TDEM}(i) = k\frac{S_{87TDEM}(i+1) - S_{87TDEM}(i)}{h} \quad (27)$$

where D_{87TDEM} represents the slope between two samples of S_{87TDEM} expressed in degrees, k is a compensation factor designed to highlight any abrupt change in the differentiation, and h represents the sample time step size. In this case, $h = 260.4166$ ms based on the 64 samples per 60 Hz cycle. The selection of the compensation factor, k, depends on the desired level of sensitivity of the algorithm. For a high value of k, the sensitivity also will be high. On the other hand, for a value of k close to one, the sensitivity of the algorithm will considerably be reduced. Therefore, a value of $k = 10$ was selected to provide a balance between sensitivity and security.

3.4. Discrimination criteria

A discrimination criteria was established to correctly differentiate transient events that do not require a trip and internal faults. This criteria is based on the degrees of D_{87TDEM} index. In steady-state the D_{87TDEM} index will take values close to zero degrees. On the other hand, if a transient event has a place, D_{87TDEM} index will achieve values in the range of 0 and -90 degrees. However, if an internal fault occurs, the D_{87TDEM} index will be close to +90 degrees.

In this sense, a C counter based on the behavior of the D_{87TDEM} index was implemented to assert the identification of the event. If the D_{87TDEM} is higher than +45 degrees, the C counter increments to 1 and compares if the C counter is higher than 3. If C counter is higher than 3, the algorithm detects an internal fault condition and sends a trip signal. Otherwise, the event is determined as a transient or a steady-state condition.

Table 1 summarizes the logic decision of the discrimination criteria. The selection of the identification threshold at +45 degrees is chosen because when an internal fault occurs, the D_{87TDEM} index starts to rapidly increase. Nevertheless, if the integrity of the transformer is considered, it is not necessary to wait until values close to +90 degrees to send a trip signal.

4. Simulation test system

The electromagnetic transient simulation program PSCAD/EMTDC was used to test the algorithm performance in the simulated three-power system shown in Fig. 3. The test system[19] includes a 230 kV, 100 MVA short-circuit equivalent source with an impedance of $15.08\,\Omega\angle 87.18°$ connected with a 230/115 kV, 100 MVA power transformer in wye-delta connection. Transmission lines are simulated in the frequency depend model with a length of 50 km. A three-phase 90 MW, 30 MVAR load and a 115 kV equivalent source with an impedance of $15.08\,\Omega\angle 87.18°$ are connected at the end of the lines 2 and 1, respectively.

The CTs used in the differential protection scheme are wye connected on both sides of the transformer. The CT ratios selected are 250:5 (C-200) and 500:5 (C-600) for the high and the low side, respectively. These CT ratios were chosen to guarantee the CTs will experience saturation during fault conditions according to[28].

5. Simulation results

The proposed algorithm was tested in a total of 2064 events. The different scenarios addressed are: inrush currents, energization with remanent flux, sympathetic inrush current, internal and external (outside the differential protection zone) faults in both sides of the transformer, overexcitation and combinations of scenarios as is show in Table 2. Every scenario was simulated 16 times with the timing of the initiation of the transient shifted in steps of one millisecond over

Table 1. Discrimination criteria

Event	Criteria
Steady-state Transient event (inrush, external fault, overexcitation)	$D_{87TDEM} < +45°$
Fault inside the differential protection zone Turn-to-turn fault	$D_{87TDEM} \geq +45°$

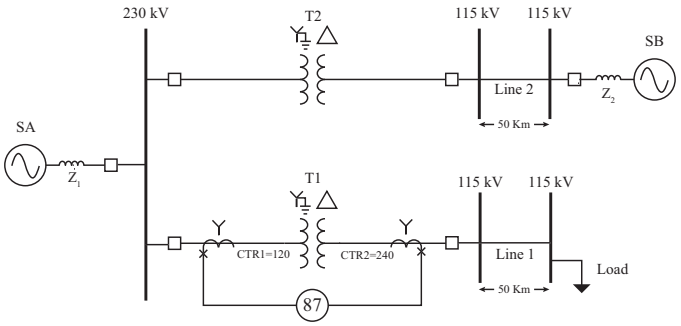

Fig. 3. Test system.

one period of 60 Hz of the voltage signal to change the incidence angle. MATLAB software was used to implement the algorithm and to process the CT secondary signals obtained from PSCAD/EMTDC with a sampling frequency of 3.84 kHz.

The results in each figure are organized as follows. Graph a) and b) are the operation and restraint currents, respectively. Graph c) and d) are the normalized operation differential, and restrain current, respectively. Graph e) shows the magnitudes of λI_{opABC} and $\lambda I_{\text{restABC}}$. Graph f) illustrates the magnitude of the $\Lambda_{87\text{TDEM}}$ index. The magnitude of the $S_{87\text{TDEM}}$ index is illustrated in graph g). Finally, graph h) presents the behavior of the $D_{87\text{TDEM}}$ index, which is expressed in degrees. The calculated index is compared with a dashed line set at 45 degrees, which represents the discrimination threshold. Also, the trip signal was added in graph h) to illustrate the instant the algorithm generates the signal to disconnect the transformer. As a comparison method, the conventional method based on phasors using Harmonic Restraint[29,2] (DFT-HR) is shown in graph i). The setting factors for DFT-HR: 87UP = 0.3, SLP = 30%, and harmonic restraint PCT = 20%[30].

5.1. Inrush current with remanent flux

Power transformers frequently are energized and de-energized for different reasons. Maintenance, external faults near to the protection zone, and internal faults are the main causes. The de-energization of the transformer will trap a remanent flux in the core of the power transformer that may cause the misoperation of the differential elements. If the remanent flux is in the same direction of the inrush current, a large current will appear at the time the transformer will be re-energized. The typical remanent flux values are on the range of 20% to 70% of the magnetic flux on steady-state. However, there are reports of values as high as 85% of remanence flux values[31]. Also, the large magnitude of the inrush currents causes the hyper-saturation of the CTs[32]. Therefore, the algorithm was tested in an event where the power transformer T1 was energized at time $t = 0.75$ s with an 85% of remanent flux, as is shown in Fig. 4. The magnitude of the $\Lambda_{87\text{TDEM}}$ and the $S_{87\text{TDEM}}$ indices were negative when the transformer was energized, and also when the CTs experienced hyper-saturation as is shown in Fig. 4f) and Fig. 4g), respectively. In consequence, Fig. 4h) shows the magnitude of the $D_{87\text{TDEM}}$ index did not cross the threshold of +45 degrees and the algorithm identified the event as a non-fault condition. On the other hand, differential elements phase A and B misoperated as is illustrated in Fig. 4i).

5.2. Internal fault

Fig. 5 shows the performance of the algorithm an in zone A-g single-phase to ground fault. The fault occurs at time $t = 1.0$ s from steady state in the HV side of the transformer. Fig. 5a) illustrates the fault impacted in phases A and B, and the CTs experienced saturation in both faulty phases. The behavior of the magnitude of the $\Lambda_{87\text{TDEM}}$ index changed from zero to positive values after the fault occurred as Fig. 5f) displays. As a result of the behavior of the positive difference of energies, the magnitude of the $S_{87\text{TDEM}}$ index also increased in a positive direction as illustrated in Fig. 5g). Therefore, the $D_{87\text{TDEM}}$ index takes values higher than the identification threshold of +45°, and the algorithm detects the event as a fault condition and sent the trip signal as is shown in Fig. 5h). The fault was detected in 1 ms. In contrast, the DFT-HR method misoperated in phases A and B, respectively as is presented in Fig. 5g). The misoperation was due to the harmonic content introduced for the CT saturation increased the restraint current at the time the fault happened. Therefore, differential elements were blocked and the transformer was not disconnected.

Table 2. Events considered in the algorithm testing.

Disturbance	Number of cases
Unloaded energizations	32
Loaded energizations	32
Energization with remanent flux (20, 30, 40, 50, 70%)	160
Transformer connection (D-Y), Y-D, Y-Y, D-D)	64
Sympathetic inrush current	32
Transformer parameter variations (voltage, connection, saturation curve, MVA rating)	128
Faults inside the differential protection zone (A-g, B-g, C-g, AB-g, BC-g, CA-g, ABC-g, AB, BC, CA, ABC)	352
Faults outside the differential protection zone (A-g, B-g, C-g, AB-g, BC-g, CA-g, ABC-g, AB, BC, CA, ABC)	352
Faults inside the differential protection zone during energization (A-g, B-g, C-g, AB-g, BC-g, CA-g, ABC-g, AB, BC, CA, ABC)	352
Faults outside the differential protection zone during energization (A-g, B-g, C-g, AB-g, BC-g, CA-g, ABC-g, AB, BC, CA, ABC)	352
Turn-to-turn faults (5, 10, 15%)	48
Total	2064

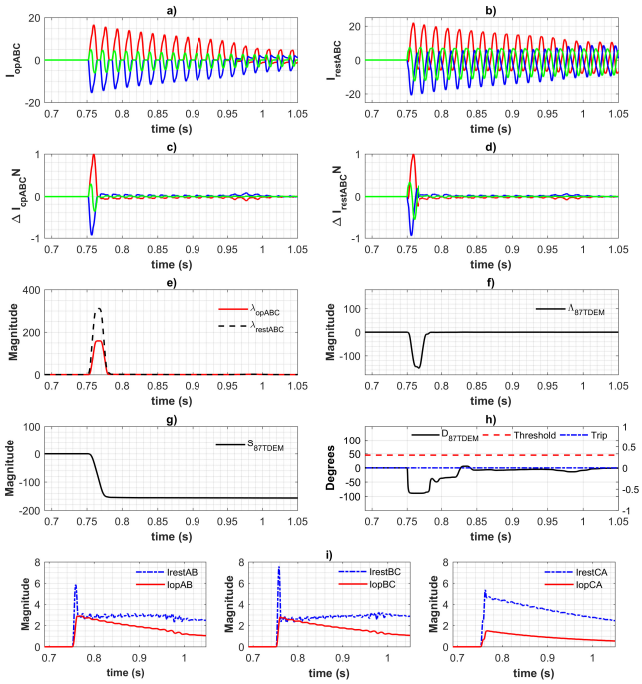

Fig. 4. Algorithm performance during an inrush current with a remanent flux of 85% in the transformer T1.

5.3. Inrush current and internal fault

The algorithm was tested when a fault inside the differential protection zone occurs after the transformer energization. The B-g single-phase to ground fault on the LV side occurred at time t = 2.0 s

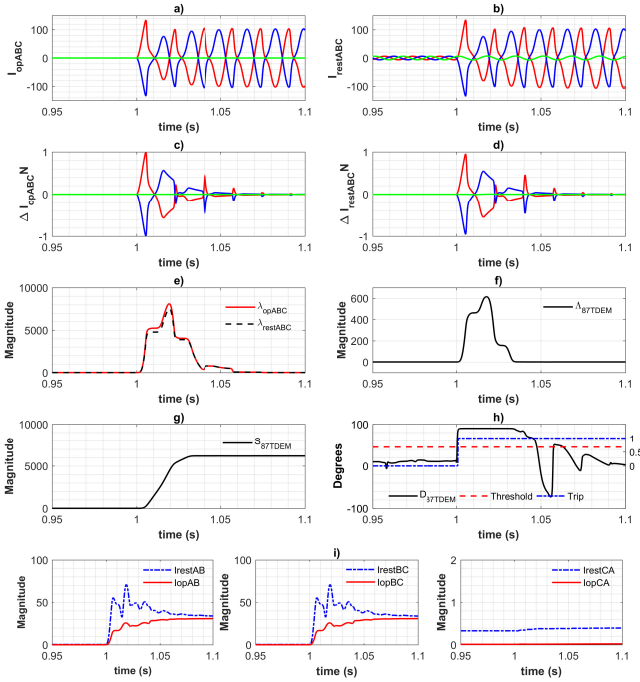

Fig. 5. Algorithm performance during an in zone A-g single-phase to ground fault in the HV side.

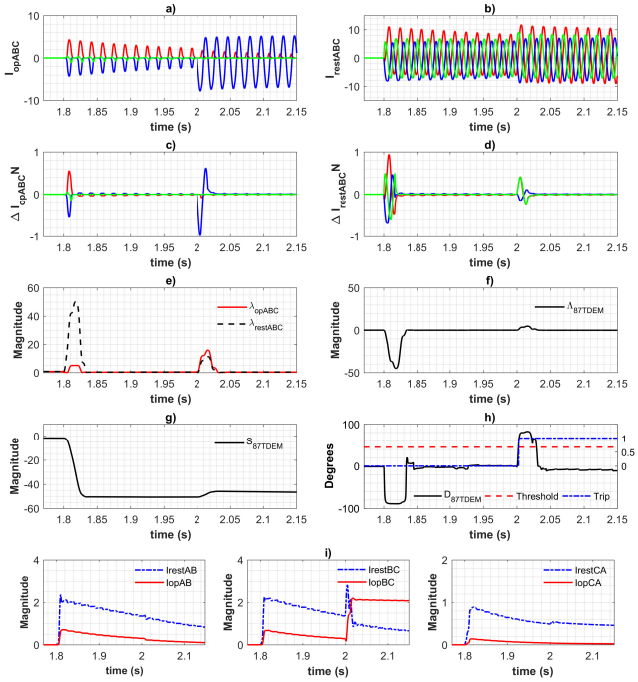

Fig. 6. Algorithm performance during an in a zone B-g single-phase to ground fault in the LV side once the transformer was energized.

once the transformer energization occurred at time t = 1.0 s. The magnitude of the Λ_{87TDEM} and S_{87TDEM} indices changed from zero to negative values when the transformer was energized. Therefore, the D_{87TDEM} index did not cross the discrimination threshold and the algorithm did not send a trip signal as is shown in Fig. 6h). However, when the internal fault occurred, the magnitude of the Λ_{87TDEM} index takes positive values and the S_{87TDEM} index increases its magnitude as is illustrated in Fig. 6f) and Fig. 6g), respectively. The changes in the magnitude of the Λ_{87TDEM} and S_{87TDEM} indices made the D_{87TDEM} index cross the discrimination threshold. As consequence, the algorithm detected a fault condition and sent the trip signal as is shown in Fig. 6h). The proposed algorithm detected the fault in 3 ms. On this event, the DFT-HR method blocked the operation of the differential elements when the inrush current happened. Nevertheless, when the internal fault occur, the harmonic content delayed the operation of the differential element phase B as is illustrated in Fig. 6i). The fault detection time by DFT-HR was 15 ms.

5.4. External fault

Ideally, the external faults should not lead the operation of differential elements because of the difference of the currents is equal to zero and the fault occurs outside of the protection zone. However, in practice, the CT saturation may cause the misoperation of differential elements due to the false large differential current generated when an external fault happens. Therefore, the algorithm was tested during an external-three phase fault in the LV side of the transformer T1 at time $t = 0.55$ s from steady-state as Fig. 7 shows. Even though the false differential current, the magnitude of the Λ_{87TDEM} and S_{87TDEM} indices takes negative values when the external three-phase fault occurred as is shown in Fig. 7f) and Fig. 7g), respectively. As a result, the D_{87TDEM} index did not exceed the discrimination threshold and the algorithm blocked the trip signal as is shown in Fig. 7h). DFT-HR method blocked the operation of the differential elements due to the high level of harmonic content in the differential currents as Fig. 7i) presents.

6. Conclusion

A new differential protection algorithm for power transformer was presented in this paper. The algorithm used the difference of the energy modes of the instantaneous differential and restraint currents using the SVD as the basis to discriminate the event. Also, the numerical integration and discrete differentiation from the difference of energies were applied to avoid the issues caused by the CT saturation and to speed up the fault detection, respectively. The algorithm was tested againts events such as inrush currents with a high percentage of remanent flux, internal and external faults, and overexcitation. Also, a laboratory transformer was used to verify the performance of the proposed algorithm. The results demonstrated a successful discrimination between the internal faults and other transient conditions. The algorithm can be applied to any transformer without requiring knowledge of the transformer parameters or the harmonic content of the differential signals. The algorithm has a fault detection time less than one cycle at 60 Hz.

References

[1] H.Bhalja, B. R. Bhavesh, P. Agarwal, and O. P. Malik, “Time-frequency decomposition based protection scheme for power transformer-simulation and experimental validation,” *IEEE Trans. on Ind. Electron.*, pp. 1–11. , 2023.

[2] R. Hamilton, “Analysis of transformer inrush current and comparison of harmonic restrain methods in power transformer protection,” *IEEE Trans. on Ind. Appl.*, vol. 49, no. 4, pp. 1890–1899, 2013.

[3] X. Sun, P. Li, X. Lin, and Y. Xiao, “Research on the influence of frequency deviation on transformer differential protection,” *IEEE International Conference on Power Science and Technology (ICPST)*, pp. 345–350, 2023.

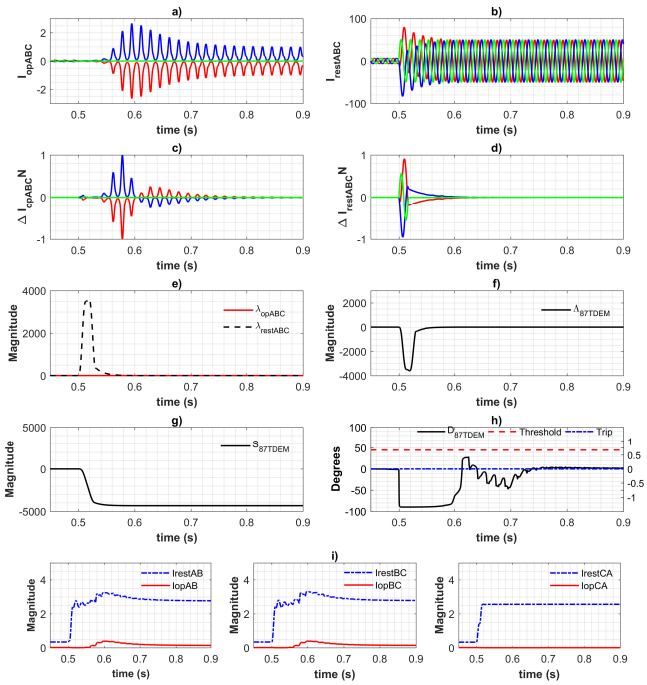

Fig. 7. Algorithm performance during an external three-phase fault in the LV side.

[4] D. Bejmert, M. Kereit, F. Mieske, W. Rebizant, K. Solak and A. Wiszniewski, "Power transformer differential protection with integral approach," *Int. J. Electr. Power Energy Syst.*, vol. 118, p. 105859, 2020.

[5] R. P. Medeiros, F. B. Costa, and K. Silva, "Power transformer differential protection using the boundary discrete wavelet transform," *IEEE Trans. on Power Del.*, vol. 31, no. 5, pp. 2083–2095, 2016.

[6] S. K. Murugan, S. P. Simon, K. Sundareswaran, P. S. R. Nayak, and N. P. Padhy, "An empirical fourier transform-based power transformer differential protection," *IEEE Trans. on Power Del.*, vol. 32, no. 1, pp. 209–218, 2017.

[7] A. M. Shah, B. R. Bhalja, and R. M. Patel, "New protection scheme for power transformer based on superimposed differential current," *IET Gener. Transm. & Distrib.*, vol. 12, no. 14, pp. 3587–3595, 2018.

[8] K. Solak, F. Mieske, and S.Schneider, "Negative-sequence current integral method for detection of turn-to-turn faults between two parallel conductors in power transformers," *Int. J. Electr. Power Energy Syst.*, vol. 141, p. 108124, 2022.

[9] A. Sahebi, and H. Samet, "Efficient method for discrimination between inrush current and internal faults in power transformers based on the non-saturation zone," *IET Gener. Transm. & Distrib.*, vol. 11, no. 6, pp. 1486–1493, 2017.

[10] W. Wu, T. Ji, M. Li, and Q. Wu, "Using mathematical morphology to discriminate between internal and inrush current of transformers," *IET Gener. Transm. & Distrib.*, vol. 10, no. 1, pp. 73–80, 2016.

[11] E. Ali, A. Helal, H. Desouki, K. Shebl, S. Abdelkader, and O.P. Malik, "Power transformer differential protection using current and voltage ratios," *Electr. Pow. Syst. Res.*, vol. 154, pp. 140–150, 2018.

[12] R. P. Medeiros and F. B. Costa, "A wavelet-based transformer differential protection: Internal fault detection during inrush conditions," *IEEE Trans. on Power Del.*, vol. 33, no. 6, pp. 2965–2977, 2018.

[13] J. P. Marques, C. Lazaro, A. P. Morais, and G. Cardos, "A reliable setting–free technique for power transformer protection based on wavelet transform," *Electr. Pow. Syst. Res.*, vol. 162, pp. 161–168, 2018.

[14] R. Afsharisefat, M.Jannati, and M. Shams, "Discrimination of inrush current and internal faults incorporating the mra and bigru techniques in power transformers," *Electr. Pow. Syst. Res.*, vol. 219, p. 109255, 2023.

[15] L. D. Simões, H.J.D. Costa, M.N.O. Aires, R.P. Medeiros, F. B. Costa, and A.S. Bretas, "A power transformer differential protection based on support vector machine and wavelet transform," *Electr. Pow. Syst. Res.*, vol. 197, p. 107297, 2021.

[16] H. Esponda, E. Vazquez, M. A. Andrade, "Differential protection in power transformers using the statistical second central moment," *The J. Eng.*, vol. 2018, no. 15, pp. 1330–1334.

[17] H. Esponda, E. Vazquez, M. A. Andrade and B. Johnson, "A setting-free differential protection for power transformers based on second central moment," *IEEE Trans. on Power Del.*, vol. doi: 10.1109/TPWRD.2018.2889471.

[18] H. Esponda, E. Vazquez, M. A. Andrade, D. Guillen, and B. Johnson, "Extended second central moment approach to detect turn-to-turn faults inpower transformers." *IET Elec. Pow. Appl.*, vol. doi: 10.1049/iet-epa.2018.5689.

[19] L. L. Zhang, Q. H. Wu, T. Y. Ji, and A. Q. Zhang, "Identification of inrush currents in power transformers based on high-order statistics," *Electr. Pow. Syst. Res.*, vol. 146, pp. 161–169, 2017.

[20] C. Mo and T.Y. Ji and L.L. Zhang and Q.H. Wu, "Equivalent statistics based inrush identification method for differential protection of power transformer," *Electr. Pow. Syst. Res.*, vol. 203, p. 107664, 2022.

[21] M. H. H. Musa, Z. He, L. Fu and Y. Deng, "A covariance indices based method for fault detection and classification in a power transmission system during power swing," *Int. J. Electr. Power Energy Syst.*, vol. 105, pp. 581–591, 2019.

[22] M. Magdon-Ismail and J. T. Purnell, "Approximating the covariance matrix of gmms with low-rank perturbations," in *Intelligent Data Engineering and Automated Learning – IDEAL 2010*, C. Fyfe, P. Tino, D. Charles, C. Garcia-Osorio, and H. Yin, Eds. Berlin, Heidelberg: Springer Berlin Heidelberg, 2010, pp. 300–307.

[23] R. L. Burden and J. D. Faires, "Singular value decomposition," in *Numerical Analysis*. USA: Brooks/Cole, 2011, ch. 9, pp. 614–625.

[24] M. P. Holmes, A. G. Gray, and C. L. Isbell, "Fast svd for large-scale matrices," 01 2007. [Online]. Available: Availableonhttps://www.researchgate.net/publication/228820785_Fast_SVD_for_large-scale_matrices

[25] D. Guillen, M. R. A. Paternina, A. Zamora, J. M. Ramirez and G. Idarraga, "Detection and classification of faults in transmission lines using the maximum wavelet singular value and euclidean norm," *IET Gener. Transm. & Distrib.*, vol. 9, no. 15, pp. 2294–2302, 2015.

[26] T. Y. Liu and K. J. Lin and H. C. Wu, "Ecg data encryption then compression using singular value decomposition," *IEEE Journal of Biomedical and Health Informatics*, vol. 22, no. 3, pp. 707–713, 2018.

[27] G. Benmouyal and J. Roberts, "Superimposed quantities: Their true nature and application in relays," in *Proc. of 26th Annual Western Protective Relay Conference*, 1999, pp. 1–18.

[28] "IEEE Guide for the Application of Current Transformers Used for Protective Relaying Purposes," Standard, 2008.

[29] B. Jafarpisheh, M. Madani, and F. Parvaresh, "Phasor estimation algorithm based on complex frequency filters for digital relaying," *IEEE Trans. Inst. Meas.*, vol. 67, no. 3, pp. 582–592, 2018.

[30] *Single-Phase Testing of the SEL-787 Harmonic Blocking and Restraint Functions*, 2011.

[31] John H. Brunke, and J. Fröhlich, "Elimination of transformer inrush currents by controlled switching?part i: Theoretical considerations," *IEEE Trans. on Power Del.*, vol. 16, no. 2, pp. 276–280, 2001.

[32] Behrendt K., Fischer N., and Labuschangne C., "Considerations for using harmonic blocking and harmonic restraint techniques on transformer differential relays," in *Proc. of 33rd Annual Western Protective Relay Conference*, 2006.